Chapter 10

Graphene/Semiconductor Nanocomposites: Preparation and Application for Photocatalytic Hydrogen Evolution

Xiaoyan Zhang and Xiaoli Cui

Additional information is available at the end of the chapter

http://dx.doi.org/10.5772/51056

1. Introduction

1.1. What is graphene?

Graphene is a flat monolayer of sp^2-bonded carbon atoms tightly packed into a two-dimensional (2D) honeycomb lattice. It is a basic building block for graphitic materials of all other dimensionalities (see Fig.1 from ref. [1]), which can be wrapped into 0D fullerene, rolled into 1D nanotubes or stacked into 3D graphite. It has high thermal conductivity (~5,000 W $m^{-1}K^{-1}$) [2], excellent mobility of charge carriers (200,000 cm^2 V^{-1} s^{-1}) [3], a large specific surface area (calculated value, 2,630 m^2 g^{-1}) [4] and good mechanical stability [5]. Additionally, the surface of graphene is easily functionalized in comparison to carbon nanotubes. Thus, graphene has attracted immense attention [1,6-8] and it shows great applications in various areas such as nanoelectronics, sensors, catalysts and energy conversion since its discovery in 2004 [9-14].

To date, various methods have been developed for the preparation of graphene via chemical or physical routes. Novoselov in 2004 firstly reported the micromechanical exfoliation method to prepare single-layer graphene sheets by repeated peeling [1]. Though the obtained graphene has high quality, micromechanical exfoliation has yielded small samples of graphene that are useful for fundamental study. Then methods such as epitaxial growth and chemical vapor deposition have been developed [15-20]. In epitaxial growth, graphene is produced by decomposition of the surface of silicon carbide (SiC) substrates *via* sublimation of silicon atoms and graphitization of remaining C atoms by annealing at high temperature (1000-1600°C). Epitaxial graphene on SiC(0001) has been demonstrated to exhibit high mobilities, especially multilayered films. Recently, single layered SiC converted graphene over a

large area has been reported and shown to exhibit outstanding electrical properties [21]. Kim et al. [17] reported the direct synthesis of large-scale graphene films using chemical vapor deposition on thin nickel layers under flowing reaction gas mixtures (CH_4:H_2:Ar = 50:65:200 standard cubic centimeters per minute), and successful transferring of them to arbitrary substrates without intense mechanical and chemical treatments. However, the graphene obtained from micromechanical exfoliation and chemical vapor deposition has insufficient functional groups, which makes its dispersion and contact with photocatalysts difficult [22]. Among the various preparation methods, the reduction of exfoliated graphene oxide (GO) was proven to be an effective and reliable method to produce graphene owing to its low cost, massive scalability, and especially that the surface properties of the obtained graphene can be adjusted via chemical modification [23]. Thus, the development of functionalized graphene-based nanocomposites has aroused tremendous attraction in many potential applications including energy storage [24], catalysis [25], biosensors [26], molecular imaging [27] and drug delivery [28].

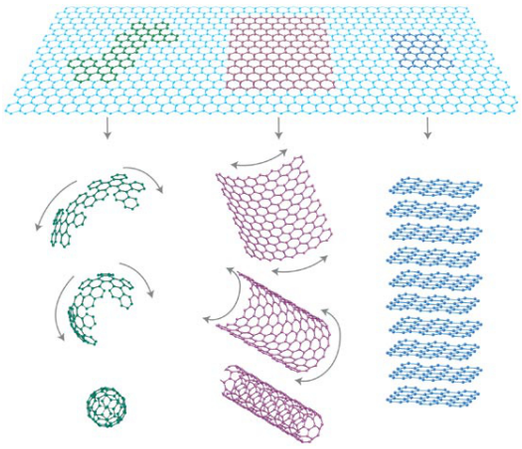

Figure 1. Mother of all graphitic forms. (from ref. [1])

1.2. What is photocatalytic hydrogen evolution?

Photocatalytic water splitting is a chemical reaction for producing hydrogen by using two major renewable energy resources, namely, water and solar energy. As the feedstocks for the reaction, water is clean, inexpensive and available in a virtually inexhaustible reserve, whereas solar energy is also infinitely available, non-polluting and appropriate for the endothermic water splitting reaction. Thus, the utilization of solar energy for the generation of hydrogen from water has been considered as an ultimate solution to solve the crisis of energy shortage and environmental degradation [29]. The following is the dissociation of the water molecule to yield hydrogen and oxygen:

$$H_2O \rightarrow 1/2O_2(g) + H_2(g); \Delta G = +237\ kJ/mol \quad (1)$$

http://dx.doi.org/10.5772/51056

This simple process has gathered a big interest from an energetic point of view because it holds the promise of obtaining a clean fuel, H_2, from a cheap resource of water [30,31]. As shown in Reaction (1), its endothermic character would require a temperature of 2500 K to obtain ca. 5% dissociation at atmospheric pressure, which makes it impractical for water splitting [32]. The free energy change for the conversion of one molecule of H_2O to H_2 and $1/2O_2$ under standard conditions corresponds to $\Delta E° = 1.23$ eV per electron transfer according to the Nernst equation. Photochemical decomposition of water is a feasible alternative because photons with a wavelength shorter than 1100 nm have the energy (1.3 eV) to split a water molecule. But, the fact is that only irradiation with wavelengths lower than 190 nm works, for that a purely photochemical reaction has to overcome a considerable energy barrier [33]. The use of a photocatalyst makes the process feasible with photons within solar spectrum since the discovery of the photoelectrochemical performance for water splitting on TiO_2 electrode by Fujishima and Honda [34].

To use a semiconductor and drive this reaction with light, the semiconductor must absorb radiant light with photon energies of larger than 1.23 eV (≤ wavelengths of 1000 nm) to convert the energy into H_2 and O_2 from water. This process must generate two electron-hole pairs per molecule of H_2 (2 × 1.23 eV = 2.46 eV). In the ideal case, a single semiconductor material having a band gap energy (E_g) large enough to split water and having a conduction band-edge energy (E_{cb}) and valence band-edge energy (E_{vb}) that straddles the electrochemical potentials $E°_{(H+/H2)}$ and $E°_{(O2/H2O)}$, can drive the hydrogen evolution reaction and oxygen evolution reaction using electrons/holes generated under illumination (see Fig. 2) [29,35].

$$H_2O + 2(h^+) \longrightarrow ½\ O_2 + 2H^+ \quad \text{(HER)}$$

$$2H^+ + 2e^- \longrightarrow H_2 \quad \text{(OER)}$$

$$H_2O \longrightarrow ½\ O_2 + H_2 \quad \Delta G = +237.2\ \text{kJ/mol}$$

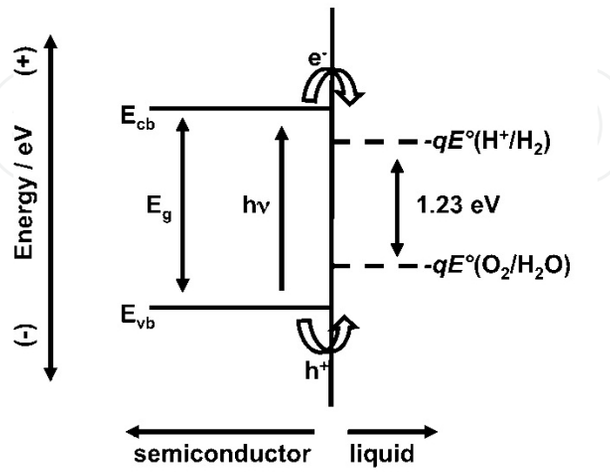

Figure 2. The mechanism of photocatalytic hydrogen evolution from water (see ref. [35])

To date, the above water splitting can be photocatalyzed by many inorganic semiconductors such as titanium dioxide (TiO_2), which was discovered in 1971 by Fujishima and Honda [34, 36]. Among the various types of widely-investigated semiconductor material, titanium dioxide (TiO_2) has been considered the most active photocatalyst due to its low cost, chemical stability and comparatively high photocatalytic efficiency [37, 38].

Frequently, sacrificial agents such as methanol [39-41], ethanol [42-44] or sulfide/sulfite [45-47] are often added into the photocatalytic system with the aim to trap photogenerated holes thus improving the photocatalytic activity for hydrogen evolution. The reaction occurred in this case is usually not the water photocatalytic decomposition reaction [48]. For example, overall methanol decomposition reaction will occur in a methanol/water system, which has a lower splitting energy than water [49]. The reaction proposed by Kawai [50] and Chen [51] was as follows:

$$CH_3OH(l) \leftrightarrow HCHO(g) + H_2(g) \qquad \Delta G_1^\circ = 64.1\ kJ/mol \tag{2}$$

$$HCHO(g) + H_2O(l) \leftrightarrow HCO_2H(l) + H_2(g) \qquad \Delta G_2^\circ = 47.8\ kJ/mol \tag{3}$$

$$HCO_2H(l) \leftrightarrow CO_2(g) + H_2(g) \qquad \Delta G_3^\circ = -95.8\ kJ/mol \tag{4}$$

With the overall reaction being

$$CH_3OH(l) + H_2O(l) \leftrightarrow CO_2(g) + 3H_2(g) \qquad \Delta G^\circ = 16.1\ kJ/mol \tag{5}$$

Consequently, it is easier for methanol decomposition in comparison to water decomposition in the same conditions.

2. Synthesis and Characterization of Graphene/Semiconductor Nanocomposite Photocatalysts

Considering its superior electron mobility and high specific surface area, graphene can be expected to improve the photocatalytic performance of semiconductor photocatalysts such as TiO_2, where graphene can act as an efficient electron acceptor to enhance the photoinduced charge transfer and to inhibit the recombination of the photogenerated electron-holes [52,53]. Thus, graphene-based semiconductor photocatalysts have also attracted a lot of attention in photocatalytic areas [7,8]. A variety of semiconductor photocatalysts have been used for the synthesis of graphene (or reduced graphene oxide) based composites. They mainly include metal oxides (e.g. TiO_2 [42-46], ZnO [61-66], Cu_2O [67], Fe_2O_3 [68], NiO [69], WO_3 [70],), metal sulfides (e.g. ZnS [71], CdS [72-77], MoS_2 [78]), metallates (e.g. Bi_2WO_6 [79],

$Sr_2Ta_2O_7$ [80], $BiVO_4$ [81], $InNbO_4$ [82] and g-Bi_2MoO_6 [83]), other nanomaterials (e.g. CdSe [84], Ag/AgCl [85,86], C_3N_4 [87,88]). The widely used synthetic strategies to prepare graphene-based photocatalysts can be divided into four types, which are sol-gel, solution mixing, in situ growth, hydrothermal and/or solvothermal methods. In fact, two or more methods are usually combined to fabricate the graphene-based semiconductor nanocomposites.

2.1. Sol -gel process

Sol-gel method is a wet-chemical technique widely used in the synthesis of graphene-based semiconductor nanocomposites. It is based on the phase transformation of a sol obtained from metallic alkoxides or organometallic precursors. For example, tetrabutyl titanate dispersed in graphene-containing absolute ethanol solution would gradually form a sol with continuous magnetic stirring, which after drying and post heat treatment changed into TiO_2/graphene nanocomposites [52,55]. The synthesis process can be schematically illuminated in Fig. 3(A) (from ref. [55]). The resulted TiO_2 nanoparticles closely dispersed on the surface of two dimensional graphene nanosheets (see Fig. 3(B) from ref. [55]). Wojtoniszak et al. [89] used a similar strategy to prepare the TiO_2/graphene nanocomposite via the hydrolysis of titanium (IV) butoxide in GO-containing ethanol solution. The reduction of GO to graphene was realized in the post heat treatment process. Farhangi et al. [90] prepared Fe-doped TiO_2 nanowire arrays on the surface of functionalized graphene sheets using a sol-gel method in the green solvent of supercritical carbon dioxide. In the preparation process, the graphene nanosheets acted as a template for nanowire growth through surface -COOH functionalities.

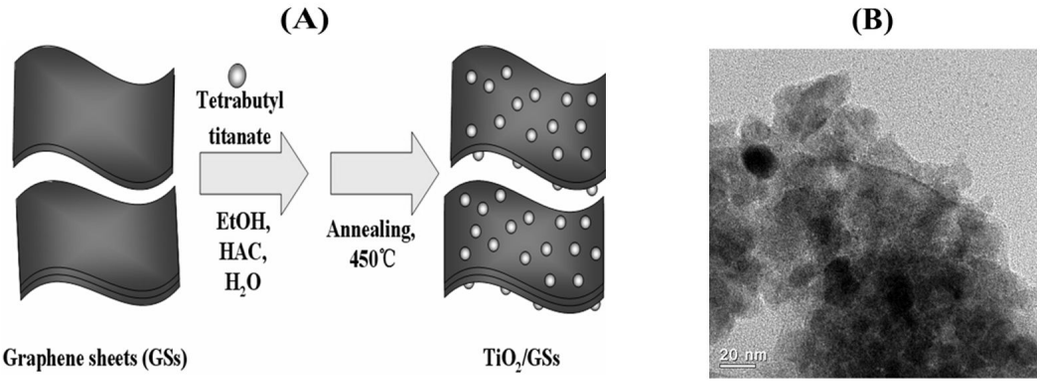

Figure 3. Schematic synthesis procedure (A) and typical TEM image of the TiO_2/graphene nanocomposites (B). (from ref. [55])

2.2. Solution mixing method

Solution mixing is a simple method to fabricate graphene/semiconductor nanocomposite photocatalysts. The oxygenated functional groups on GO facilitate the uniform distribution of photocatalysts under vigorous stirring or ultrasonic agitation [91]. Graphene-based nanocomposites can be obtained after the reduction of GO in the nanocomposite.

For example, Bell et al. [92] fabricated TiO_2/graphene nanocomposites by ultrasonically mixing TiO_2 nanoparticles and GO colloids together, followed by ultraviolet (UV)-assisted photocatalytic reduction of GO to graphene. Similarly, GO dispersion and N-doped $Sr_2Ta_2O_7$ have been mixed together, followed by reduction of GO to yield $Sr_2Ta_2O_{7-x}N_x$/graphene nanocomposites under xenon lamp irradiation [80]. Graphene-CdSe quantum dots nanocomposites have also been synthesized by Geng et al. [84]. In this work, pyridine-modified CdSe nanoparticles were mixed with GO sheets, where pyridine ligands were considered to provide π-π interactions for the assembly of CdSe nanoparticles on GO sheets. They thought that pyridine ligands could provide π-π interactions for the assembly of CdSe nanoparticles capped with pyridine on GO sheets. Paek et al. [93] prepared the SnO_2 sol by hydrolysis of $SnCl_4$ with NaOH, and then the prepared graphene dispersion was mixed with the sol in ethylene glycol to form the SnO_2/graphene nanocomposite. Most recently, Liao et al. [88] fabricated GO/g-C_3N_4 nanocomposites via sonochemical approach, which was realized by adding g-C_3N_4 powder into GO aqueous solution followed by ultrasonication for 12 h and then drying at 353 K.

2.3. Hydrothermal/solvothermal approach

The hydrothermal/solvothermal process is another effective method for the preparation of semiconductor/graphene nanocomposites, and it has unique advantage for the fabrication of graphene-based photocatalysts. In this process, semiconductor nanoparticles or their precursors are loaded on the GO sheets, where GO are reduced to graphene simultaneously with or without reducing agents or in the following step.

For example, Zhang et al. [54] synthesized graphene-TiO_2 nanocomposite photocatalyst by hydrothermal treatment of GO sheets and commercial TiO_2 powders (Degussa P25) in an ethanol-water solvent to simultaneously achieve the reduction of GO and the deposition of P25 on the carbon substrate. In order to increase the interface contact and uniform distribution of TiO_2 nanoparticles on graphene sheets, a one-pot hydrothermal method was applied using GO and $TiCl_4$ in an aqueous system as the starting materials [94]. Wang et al. [95] used a one-step solvothermal method to produce graphene-TiO_2 nanocomposites with well-dispersed TiO_2 nanoparticles by controlling the hydrolysis rate of titanium isopropoxide. Li and coworkers [74] synthesized graphene-CdS nanocomposites by a solvothermal method in which graphene oxide (GO) served as the support and cadmium acetate ($Cd(Ac)_2$) as the CdS precursor. Reducing agents can also be added into the reaction system. Recently, Shen et al. [96] added glucose as the reducing agent in the one-pot hydrothermal method for preparation of graphene-TiO_2 nanocomposites. Ternary nanocomposites system can also be obtained by a two-step hydrothermal process. Xiang et al. [42] prepared TiO_2/MoS_2/graphene hybrid by a two-step hydrothermal method.

Furthermore, some solvothermal experiments can result in the semiconductor nanoparticles with special morphology on graphene sheets. Shen et al. [97] reported an ionic liquid-assisted one-step solvothermal method to yield TiO_2 nanoparticle-graphene composites with a dendritic structure as a whole. Li et al. [78] synthesized MoS_2/graphene hybrid by a one-step solvothermal reaction of $(NH_4)_2MoS_4$ and hydrazine in a N, N dimethylformamide (DMF)

http://dx.doi.org/10.5772/51056

solution of GO. During this process, the $(NH_4)_2MoS_4$ precursor was reduced to MoS_2 on GO sheets and the GO simultaneously to RGO by reducing agent of hydrazine. The existence of graphene can change the morphology of the resulted MoS_2 in the graphene/MoS_2 nanocomposite in comparison to pure MoS_2 (see Fig. 4 from ref. [78]). Ding et al. [98] reported graphene-supported ultrathin anatase TiO_2 nanosheets with exposed (001) high-energy facets by a simple solvothermal method. In this process, anatase TiO_2 nanosheets directly grew from titanium (IV) isopropoxide onto the GO support during the solvothermal growth of TiO_2 nanocrystals in isopropyl alcohol solvent, and then GO was reduced to graphene via a post thermal treatment under N_2/H_2 to finally obtain the graphene-TiO_2 nanocomposite.

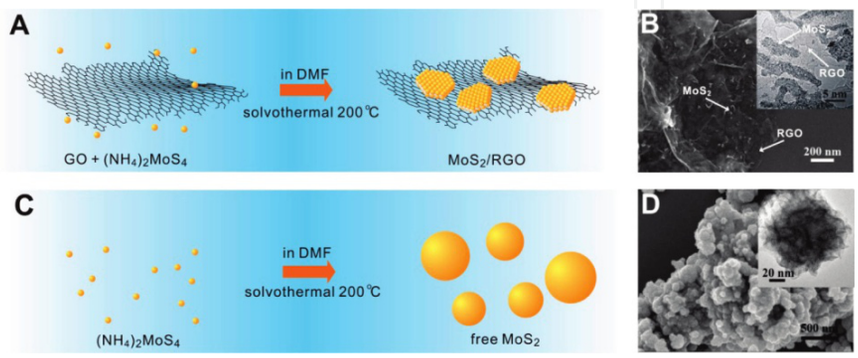

Figure 4. Synthesis of MoS_2 in solution with and without graphene sheets. (A) Schematic solvothermal synthesis with GO sheets. (B) SEM and (inset) TEM images of the MoS_2/graphene hybrid. (C) Schematic solvothermal synthesis without any GO sheets, resulting in large, free MoS_2 particles. (D) SEM and (inset) TEM images of the free particles. (from ref. [78])

2.4. *In situ* growth strategy

In situ growth strategy can afford efficient electron transfer between graphene and semiconductor nanoparticles through their intimate contact, which can also be realized by hydrothermal and/or solvothermal method. The most common precursors for graphene and metal compound are functional GO and metal salts, respectively. The presence of epoxy and hydroxyl functional groups on graphene can act as the heterogeneous nucleation sites and anchor semiconductor nanoparticles avoiding the agglomeration of the small particles [99]. Zhu et al. [100] reported a one-pot water-phase approach for synthesis of graphene/TiO_2 composite nanosheets using $TiCl_3$ as both the titania precursor and the reducing agent. Lambert et al. [101] also reported the *in situ* synthesis of nanocomposites of petal-like TiO_2-GO by the hydrolysis of TiF_4 in the presence of aqueous dispersions of GO, followed by post chemical or thermal treatment to produce TiO_2-graphene hybrids. With the concentration of graphene oxide high enough and stirring off, long-range ordered assemblies of TiO_2-GO sheets were obtained because of self-assembly. Guo et al. [102] synthesized TiO_2/graphene nanocomposite sonochemically from $TiCl_4$ and GO in ethanol-water system, followed by a hydrazine treatment to reduce GO into graphene. The average size of the TiO_2 nanoparticles was controlled at around 4-5 nm on the sheets, which is attributed to the pyrolysis and condensation of the dissolved $TiCl_4$ into TiO_2 by ultrasonic waves.

3. Applications of Graphene-based Semiconductor Nanocomposites for Photocatalytic Hydrogen Evolution

Hydrogen is regarded as an ultimate clean fuel in the future because of its environmental friendliness, renewability, high-energy capability, and a renewable and green energy carrier [103-105]. Using solar energy to produce hydrogen from water splitting over semiconductor is believed to be a good choice to solve energy shortage and environmental crisis [106,107]. Various semiconductor photocatalysts have been reported to have the performance of photocatalytic hydrogen evolution from water. However, the practical application of this strategy is limited due to the fast recombination of photoinduced electron-holes and low utilization efficiency of visible light. Because of the superior electrical property of graphene, there is a great interest in combining semiconductor photocatalysts with graphene to improve their photocatalytic H_2 production activity [8,54].

Zhang et al. firstly reported the photocatalytic activity of TiO_2/graphene nanocomposites for hydrogen evolution [55]. The influences of graphene loading contents and calcination atmosphere on the photocatalytic performance of the sol-gel prepared TiO_2-graphene composites have been investigated, respectively. The results show that the photocatalytic performance of the sol-gel prepared TiO_2/5.0wt%graphene nanocomposites was much higher than that of P25 for hydrogen evolution from Na_2S-Na_2SO_3 aqueous solution under UV-Vis light irradiation. Yu and his coworkers studied the photocatalytic performance of graphene/TiO_2 nanosheets composites for hydrogen evolution from methanol/water solution (see Fig. 5 from ref. [108]). They investigated the effect of TiO_2 precursor on the photocatalytic performance of the synthesized nanocomposites under UV light irradiation. Enhanced photocatalytic H_2 production was observed for the prepared graphene/TiO_2 nanosheets composite in comparison to that of graphene/P25 nanoparticles composites as shown in Figure 6 (see ref. [108]).

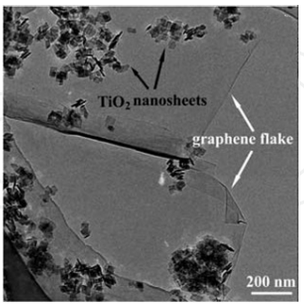

Figure 5. TEM images of the graphene/TiO_2 nanosheets nanocomposite. (from ref. [108])

Fan et al. [58] systematically studied the influence of different reduction approaches on the efficiency of hydrogen evolution for P25/graphene nanocomposites prepared by UV-assisted photocatalytic reduction, hydrazine reduction, and a hydrothermal reduction method. The photocatalytic results show that the P25/graphene composite prepared by the hydrothermal method possessed the best performance for hydrogen evolution from methanol aqueous sol-

http://dx.doi.org/10.5772/51056

ution under UV-Vis light irradiation, followed by P25/graphene-photo reduction and P25/graphene-hydrazine reduction, respectively. The maximum value exceeds that of pure P25 by more than 10 times. Figure 7 shows the morphology and XRD patterns of the one-pot hydrothermal synthesized TiO_2/graphene composites [94]. It can be observed that TiO_2 nanoparticles dispersed uniformly on graphene sheets as shown in Figure 7(A). The TiO_2/graphene nanocomposites are composed mainly anatase TiO_2 confirmed from the XRD results as shown in Figure 7(B).

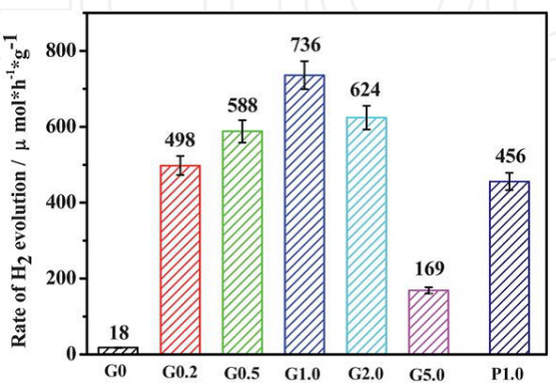

Figure 6. Comparison of the photocatalytic activity of the G0, G0.2, G0.5, G1.0, G2.0, G5.0 and P1.0 samples for the photocatalytic H_2 production from methanol aqueous solution under UV light irradiation. (Gx, x is the weight percentage of graphene in the graphene/TiO_2 nanosheets nanocomposites; P1.0 is the graphene/P25 nanocomposite with 1.0wt% graphene.) (from ref. [108])

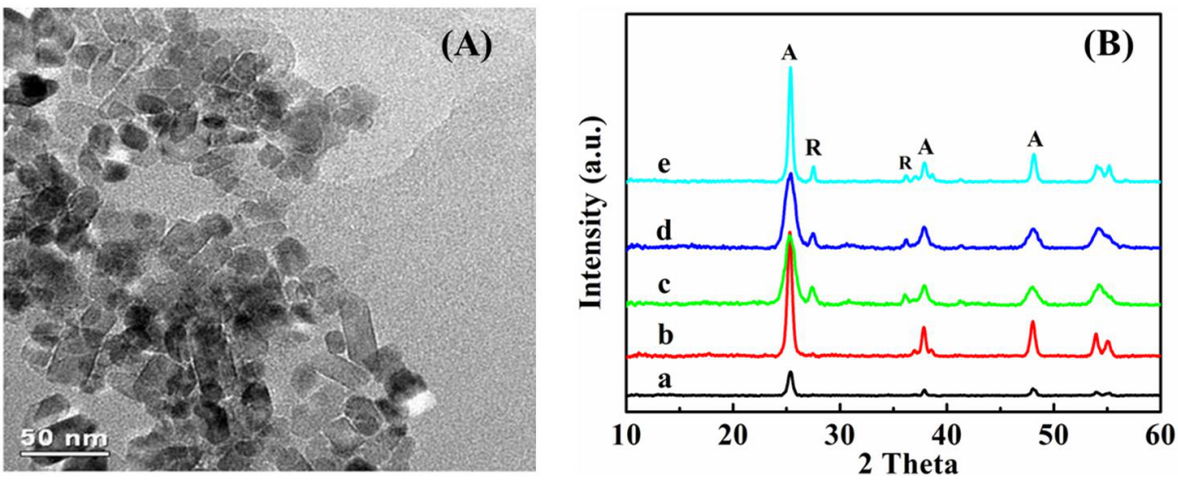

Figure 7. Typical TEM image (A) and XRD patterns (B) of the one-pot hydrothermal synthesized TiO_2/graphene nanocomposites. (from ref. [94])

The CdS/graphene nanocomposites have also attracted many attentions for photocatalytic hydrogen evolution. Li et al. [74] investigated the visible-light-driven photocatalytic activity of CdS-cluster-decorated graphene nanosheets prepared by a solvothermal method for hydrogen production (see Fig. 8). These nanosized composites exhibited higher H_2-production

rate than that of pure CdS nanoparticles. The hydrogen evolution rate of the nanocomposite with graphene content as 1.0 wt % and Pt 0.5 wt % was about 4.87 times higher than that of pure CdS nanoparticles under visible-light irradiation.

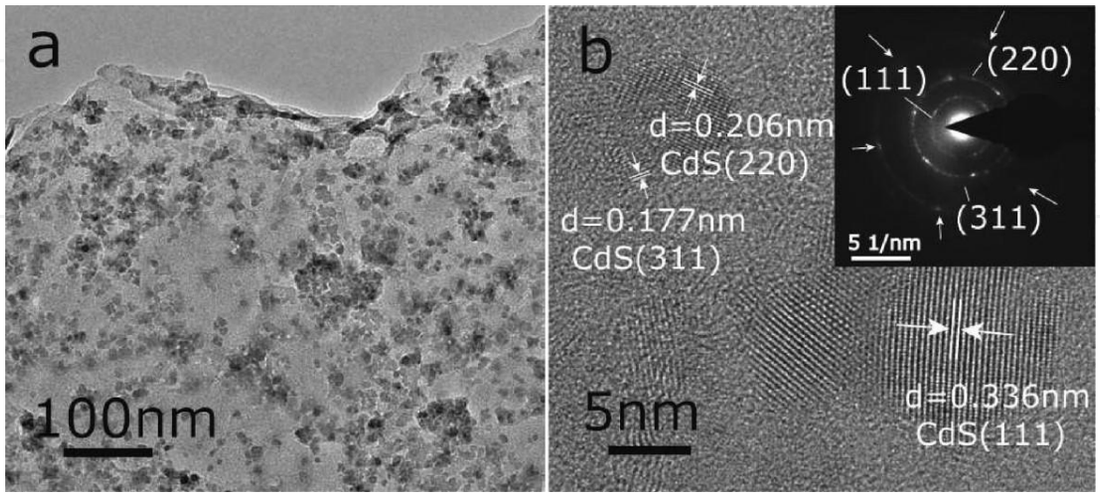

Figure 8. a) TEM and (b) HRTEM images of sample GC1.0, with the inset of (b) showing the selected area electron diffraction pattern of graphene sheet decorated with CdS clusters. (GC1.0 was synthesized with the weight ratios of GO to $Cd(Ac)_2$ $2H_2O$ as 1.0%). (see ref. [74])

4. Mechanism of the Enhanced Photocatalytic Performance for H_2 Evolution

It is well-known that graphene has large surface area, excellent conductivity and high carriers mobility. The large surface of graphene sheet possesses more active adsorption sites and photocatalytic reaction centers, which can greatly enlarge the reaction space and enhance photocatalytic activity for hydrogen evolution [74,110].

Excellent conductivity and high carriers mobility of graphene sheets facilitate that graphene attached to semiconductor surfaces can efficiently accept and transport electrons from the excited semiconductor, suppressing charge recombination and improving interfacial charge transfer processes. To confirm this hypothesis, the impedance spectroscopy (EIS) of the graphene/TiO_2 nanocomposite films was given as shown in Figure 9 (see ref. [108]). In the EIS measurements, by applying an AC signal to the system, the current flow through the circuit can be modeled to deduce the electrical behavior of different structures within the system. Figure 9 shows the conductance and capacitance as a function of frequency for FTO electrodes coated with TiO_2 and reduced graphene oxide (RGO)-TiO_2 with different RGO content (0.5, 1.0, and 1.5 mg) using a custom three-electrode electrochemical cell with a gold wire counter electrode and Ag/AgCl reference electrode in 0.01M H_2SO_4 electrolyte in a frequency range from 1 mHz to 100 kHz. Information about the films themselves is obtained from the region between 1 mHz and 1 kHz. At frequencies below 100 Hz, the conductivity is the

http://dx.doi.org/10.5772/51056

films themselves, and at ultralow frequencies (1 mHz), the conductivity is dominated by the interface between the film and the FTO. So it can be seen that the RGO in the nanocomposites films not only enhances conductivity within the film but also the conduction between the film and the FTO substrate. The same results are obtained from the inset Nyquist plots, where the radius of each arc is correlated with the charge transfer ability of the corresponding film; the larger the radius the lower the film's ability to transfer charge. The luminescence decay spectra in Figure 10 (see ref. [109]) indicate the electron transfer from photoexcited CdS nanoparticles into modified graphene (mG), thereby leading to decrease of emission lifetime from CdS to CdS-mG, further confirming that graphene can improve the charge separation and suppress the recombination of excited carriers.

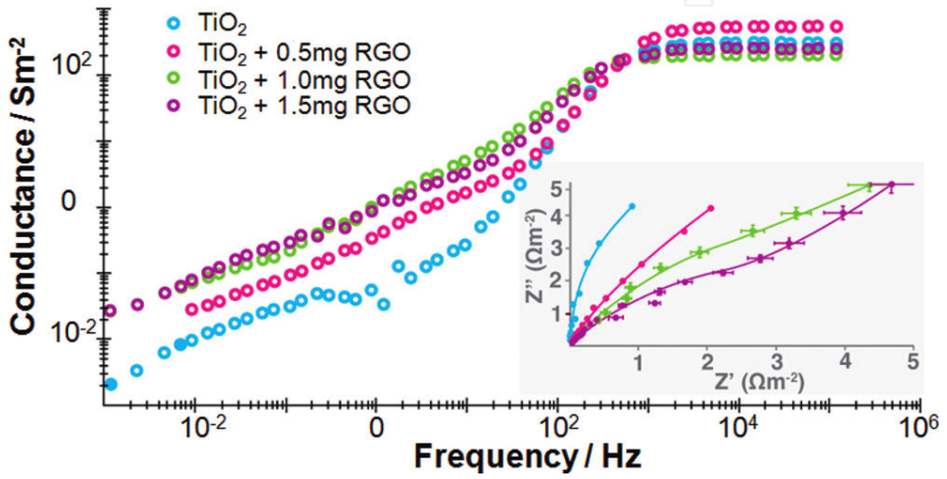

Figure 9. EIS conductance plot of TiO_2 and RGO- TiO_2 films. (Inset) Nyquist plots of the same films. (see from ref. [109])

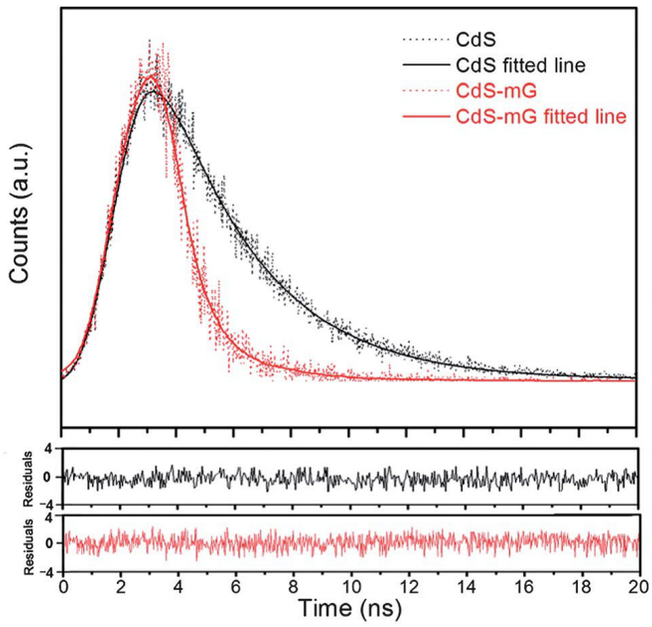

Figure 10. Time-resolved fluorescence decays of the CdS and CdS-mG solution at the 20 ns scanning range. Excited wavelength is at 355 nm, and emission wavelength is 385 nm. Bold curves are fitted results. (mG is modified graphene) (see ref. [110])

Figure 11 shows (a) the schematic illustration for the charge transfer and separation in the graphene/TiO_2 nanosheets system under UV light irradiation and (b) the proposed mechanism for photocatalytic H_2-production under UV light irradiation. Normally, the photogenerated charge carriers quickly recombine with only a small fraction of the electrons and holes participating in the photocatalytic reaction, resulting in low conversion efficiency [110,111]. When graphene was introduced into TiO_2 nanocomposite, the photogenerated electrons on the conduction band (CB) of TiO_2 tend to transfer to graphene sheets, suppressing the recombination of photogenerated electron-holes.

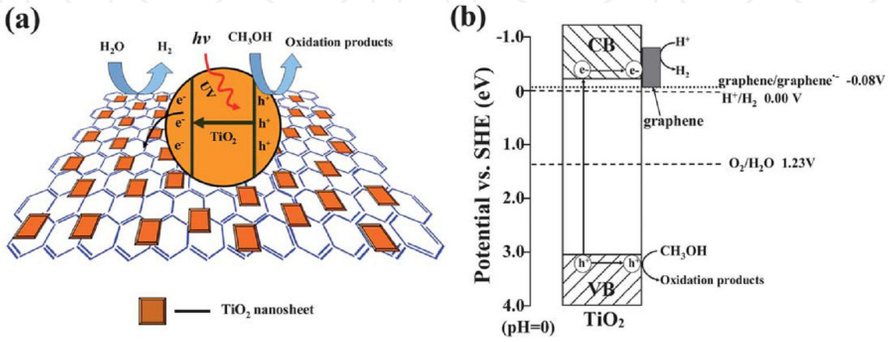

Figure 11. a) Schematic illustration for the charge transfer and separation in the graphene-modified TiO_2 nanosheets system under UV light irradiation; (b) proposed mechanism for photocatalytic H_2-production under UV light irradiation. (from ref. [108])

Moreover, a red shift of the absorption edge of semiconductor photocatalyst upon modified by graphene (or reduced graphene oxide) was observed (see Fig. 12 from ref. [58]) by many researchers from the diffuse reflectance UV-Vis spectroscopy, which was proposed to be ascribed to the interaction between semiconductor and graphene (or reduced graphene oxide) in the nanocomposites [55,58,73,108,112]. Therefore, it can be inferred that the introduction of graphene in semiconductor photocatalysts is effective for the visible-light response of the corresponding nanocomposite, which leads to more efficient utilization of the solar energy.

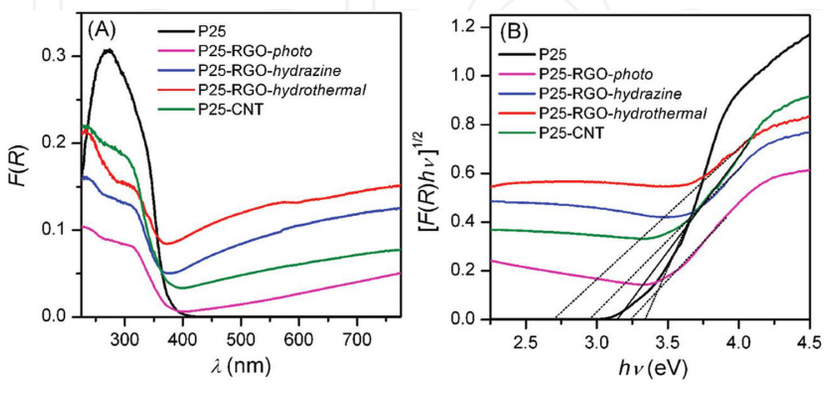

Figure 12. A) Diffuse reflectance UV-Vis spectra of P25, P25-RGO nanocomposites (P25/RGO = 1/0.2) prepared by different methods, and P25-CNT composite (P25/CNT = 1/0.3). (B) Corresponding plot of transformed Kubelka-Munk function versus the energy of the light. (see from ref. [58])

http://dx.doi.org/10.5772/51056

The above results suggest an intimate interaction between semiconductor photocatalysts and graphene sheets is beneficial for the visible light absorption and separation of photogenerated electron and hole pairs, leading to enhanced photocatalytic performance for hydrogen evolution.

5. Summary and Perspectives

In summary, graphene can be coupled with various semiconductors to form graphene-semiconductor nanocomposites due to its unique large surface area, high conductivity and carriers mobility, easy functionalization and low cost. The unique properties of graphene have opened up new pathways to fabricate high-performance photocatalysts. In this chapter, we have summarized the various fabrication methods such as solution mixing, sol gel, in situ growth, and hydrothermal/solvothermal methods that have been developed for fabricating the graphene-based semiconductor photocatalysts. These composites have shown potential applications in energy conversion and environmental treatment areas.

Although great progress has been achieved, challenges still exist in this area and further developments are required. The first challenge is that the quality-control issues of graphene still need to be addressed. Graphene oxide is believed to be a better starting material than pure graphene to form nanocomposite with semiconductor photocatalysts. However, reduction of graphene oxide into graphene usually can bring defects and impurity simultaneously. Thus, new synthesis strategies have to be developed to fabricate high-performance graphene-semiconductor composites. The second one is the semiconductor photocatalysts. The introduction of graphene into the nanocomposites mainly acts to promote the separation of charge carriers and transport of photogenerated electrons. The performance of photocatalysts is highly dependent on the semiconductor photocatalysts and their surface structures such as the morphologies and surface states. Therefore, the development of novel photocatalysts is required. Furthermore, the underlying mechanism of the photocatalytic enhancement by the graphene-based semiconductor nanocomposites is partly unclear. For example, whether graphene can change the band gap of the semiconductor photocatalysts, and whether graphene can truly sensitize semiconductor photocatalysts. Nevertheless, there are still many challenges and opportunities for graphene-based semiconductor nanocomposites and they are still expected to be developed as potential photocatalysts to address various environmental and energy-related issues.

Acknowledgements

This work is supported by the National Science Foundation of China (No. 21273047) and National Basic Research Program of China (Nos. 2012CB934300, 2011CB933300), the Shanghai Science and Technology Commission (No. 1052nm01800) and the Key Disciplines Innovative Personnel Training Plan of Fudan University.

Author details

Xiaoyan Zhang and Xiaoli Cui*

*Address all correspondence to: xiaolicui@fudan.edu.cn

Department of Materials Sciences, Fudan University, Shanghai, 200433, China

References

[1] Novoselov, K. S., Geim, A. K., Morozov, S. V., Jiang, D., Zhang, Y., Dubonos, S. V., Grigorieva, I. V., & Firsov, A. A. (2004). *Science*, 306, 666.

[2] Balandin, A. A., Ghosh, S., Bao, W. Z., Calizo, I., Teweldebrhan, D., Miao, F., & Lau, C. N. (2008). *Nano Lett.*, 8, 902-907.

[3] Bolotin, K. I., Sikes, K. J., Jiang, Z., Klima, M., Fudenberg, G., Hone, J., Kim, P., & Stormer, H. L. (2008). *Solid State Commun.*, 146, 351-355.

[4] Stoller, M. D., Park, S., Zhu, Y., An, J., & Ruoff, R. S. (2008). *Nano Lett.*, 8, 3498-3502.

[5] Lee, C., Wei, X., Kysar, J. W., & Hone, J. (2008). *Science*, 321, 385-388.

[6] Pyun, J. (2011). *Angew. Chem. Int. Ed.*, 50, 46.

[7] Xiang, Q. J., Yu, J. G., & Jaroniec, M. (2012). *Chem. Soc. Rev.*, 41(2), 782-796.

[8] An, X. Q., & Yu, J. C. (2011). *RSC Advances*, 1, 1426-1434.

[9] Wei, D., & Liu, Y. (2010). *Adv. Mater.*, 22, 3225.

[10] Allen, M. J., Tung, V. C., & Kaner, R. B. (2010). *Chem. Rev.*, 110, 132.

[11] Chen, J. S., Wang, Z., Dong, X., Chen, P., & Lou, X. W. (2011). *Nanoscale*, 3, 2158.

[12] Yi, J., Lee, J. M., & Park, W. I. (2011). *Sens. Actuators*, B155, 264.

[13] Fan, Y., Lu, H. T., Liu, J. H., Yang, C. P., Jing, Q. S., Zhang, Y. X., Yang, X. K., & Huang, K. J. (2011). *Colloids Surf.*, B83, 78.

[14] Johnson, J., Behnam, A., Pearton, S. J., & Ural, A. (2010). *Adv. Mater.*, 22, 4877.

[15] Lin, Y. M., Dimitrakopoulos, C., Jenkins, K. A., Farmer, D. B., Chiu, H. Y., & Grill, A. (2010). *Science*, 327, 662.

[16] de Heer, W. A., Berger, C., Wu, X., First, P. N., Conrad, E. H., Li, X., Li, T., Sprinkle, M., Hass, J., Sadowski, M. L., Potemski, M., & Martinez, G. (2007). *Solid State Commun.*, 143, 92.

[17] Kim, K. S., Zhao, Y., Jang, H., Lee, S. Y., Kim, J. M., Kim, K. S., Ahn, J. H., Kim, P., Choi, J. Y., & Hong, B. H. (2009). *Nature*, 457, 706-710.

[18] Sutter, P. W., Flege, J. I., & Sutter, E. A. (2008). *Nature Mater.*, 7, 406-411.

[19] Reina, A., Jia, X. T., Ho, J., Nezich, D., Son, H., Bulovic, V., Dresselhaus, M. S., & Kong, J. (2009). *Nano Lett.*, 9(1), 30-35.

[20] Dato, A., Radmilovic, V., Lee, Z., Phillips, J., & Frenklach, M. (2008). *Nano Lett.*, 8, 2012-2016.

[21] Wu, X., Hu, Y., Ruan, M., Madiomanana, N. K., Hankinson, J., Sprinkle, M., Berger, C., & de Heer, W. A. (2009). *Appl. Phys. Lett.*, 95, 223108.

[22] Cui, X., Zhang, C., Hao, R., & Hou, Y. (2011). *Nanoscale*, 3, 2118.

[23] Park, S., & Ruoff, R. S. (2009). *Nat. Nanotechnol.*, 4, 217.

[24] Wang, K., Ruan, J., Song, H., Zhang, J., Wo, Y., Guo, S., & Cui, D. (2011). *Nanoscale Res. Lett.*, 6, 8.

[25] Wang, Q., Guo, X., Cai, L., Cao, Y., Gan, L., Liu, S., Wang, Z., Zhang, H., & Li, L. (2011). *Chem. Sci.*, 2, 1860-1864.

[26] Park, S., Mohanty, N., Suk, J. W., Nagaraja, A., An, J., Piner, R. D., Cai, W., Dreyer, D. R., Berry, V., & Ruoff, R. S. (2010). *Adv. Mater.*, 22, 1736.

[27] Cai, W. B., & Chen, X. Y. (2007). *Small*, 3, 1840.

[28] Akhavan, O., Ghaderi, E., & Esfandiar, A. (2011). *J. Phys. Chem.*, B115, 6279.

[29] Osterloh, F. E. (2008). *Chem. Mater.*, 20, 35-54.

[30] Serpone, N., Lawless, D., & Terzian, R. (1992). *Sol. Energy*, 49, 221.

[31] Hernández-Alonso, M. D., Fresno, F., Suárez, S., & Coronado, J. M. (2009). *Energy Environ. Sci.*, 2, 1231-1257.

[32] Kodama, T., & Gokon, N. (2007). *Chem. Rev.*, 107, 4048.

[33] Gonzalez, M. G., Oliveros, E., Worner, M., & Braun, A. M. (2004). *Photochem. Photobiol.*, C5(3), 225.

[34] Fujishima, A., & Honda, K. (1972). *Nature*, 238(5358), 37.

[35] Walter, M. G., Warren, E. L., McKone, J. R., Boettcher, S. W., Mi, Q. X., Santori, E. A., & Lewis, N. S. (2010). *Chem. Rev.*, 110(11), 6446-6473.

[36] Fujishima, A., & Honda, K. B. (1971). *Chem. Soc. Jpn.*, 44(4), 1148.

[37] Ni, M., Leung, M. K. H., Dennis, Y. C., Leung, K., & Sumathy, . (2007). *Renewable and Sustainable Energy Reviews*, 11, 401-425.

[38] Hoffmann, M. R., Martin, S. T., Choi, W., & Bahnemann, D. W. (1995). *Chem. Rev.*, 95, 69-96.

[39] Wang, L., & Wang, W. Z. (2012). *Int. J. Hydrogen Energy*, 37, 3041-3047.

[40] Yang, X. Y., Salzmann, C., Shi, H. H., Wang, H. Z., Green, M. L. H., & Xiao, T. C. (2008). *J. Phys. Chem.*, A112, 10784-10789.

[41] Sreethawong, T., Laehsalee, S., & Chavadej, S. (2009). *Catalysis Communications*, 10, 538-543.

[42] Xiang, Q. J., Yu, J. G., & Jaroniec, M. (2012). *J. Am. Chem. Soc.*, 134, 6575.

[43] Wang, Y. Q., Zhang, Z. J., Zhu, Y., Li, Z. C., Vajtai, R., Ci, L. J., & Ajayan, P. M. (2008). *ACS Nano*, 2(7), 1492-1496.

[44] Eder, D., Motta, M., & Windle, A. H. (2009). *Nanotechnology*, 20, 055602.

[45] Yang, H. H., Guo, L. J., Yan, W., & Liu, H. T. (2006). *J. Power Sources*, 159, 1305-1309.

[46] Yao, Z. P., Jia, F. Z., Tian, S. J., Li, C. X., Jiang, Z. H., & Bai, X. F. (2010). *Appl. Mater. Interfaces*, 2(9), 2617-2622.

[47] Jang, J. S., Hong, S. J., Kim, J. Y., & Lee, J. S. (2009). *Chemical Physics Letters*, 475, 78-81.

[48] Chen, T., Feng, Z. C., Wu, G. P., Shi, J. Y., Ma, G. J., Ying, P. L., & Li, C. (2007). *J. Phys. Chem.*, C111, 8005-8014.

[49] Lin, W. C., Yang, W. D., Huang, I. L., Wu, T. S., & Chung, Z. J. (2009). *Energy & Fuels*, 23, 2192-2196.

[50] Kawai, T., & Sakata, T. (1980). *J. Chem. Soc. Chem. Commun.*, 15, 694-695.

[51] Chen, J., Ollis, D. F., Rulkens, W. H., & Bruning, H. (1999). *Water. Res.*, 33, 669-676.

[52] Zhang, X. Y., Li, H. P., & Cui, X. L. (2009). *Chinese Journal of Inorganic Chemistry*, 25(11), 1903-1907.

[53] Lightcap, I. V., Kosel, T. H., & Kamat, P. V. (2010). *Nano Lett.*, 10, 577.

[54] Zhang, H., Lv, X. J., Li, Y. M., Wang, Y., & Li, J. H. (2010). *ACS Nano*, 4, 380.

[55] Zhang, X. Y., Li, H. P., Cui, X. L., & Lin, Y. H. (2010). *J. Mater. Chem.*, 20, 2801.

[56] Du, J., Lai, X. Y., Yang, N. L., Zhai, J., Kisailus, D., Su, F. B., Wang, D., & Jiang, L. (2011). *ACS Nano*, 5, 590.

[57] Zhou, K. F., Zhu, Y. H., Yang, X. L., Jiang, X., & Li, C. Z. (2011). *New J. Chem.*, 35, 353.

[58] Fan, W. Q., Lai, Q. H., Zhang, Q. H., & Wang, Y. (2011). *J. Phys. Chem.*, C115, 10694-10791.

[59] Liang, Y. T., Vijayan, B. K., Gray, K. A., & Hersam, M. C. (2011). *Nano Lett.*, 11, 2865.

[60] Zhang, L. M., Diao, S. O., Nie, Y. F., Yan, K., Liu, N., Dai, B. Y., Xie, Q., Reina, A., Kong, J., & Liu, Z. F. (2011). *J. Am. Chem. Soc.*, 133, 2706.

[61] Li, B. J., & Cao, H. Q. (2011). *J. Mater. Chem.*, 21, 3346.

[62] Williams, G., & Kamat, P. V. (2009). *Langmuir*, 25, 13869.

[63] Lee, J. M., Pyun, Y. B., Yi, J., Choung, J. W., & Park, W. I. (2009). *J. Phys. Chem.*, C113, 19134.

[64] Akhavan, O. (2010). *ACS Nano*, 4, 4174.

[65] Xu, T. G., Zhang, L. W., Cheng, H. Y., & Zhu, Y. F. (2011). *Appl. Catal.*, B101, 382.

[66] Akhavan, O. (2011). *Carbon*, 49, 11.

[67] Xu, C., Wang, X., & Zhu, J. W. (2008). *J. Phys. Chem.*, C112, 19841.

[68] Morishige, K., & Hamada, T. (2005). *Langmuir*, 21, 6277.

[69] Wang, D. H., Kou, R., Choi, D., Yang, Z. G., Nie, Z. M., Li, J., Saraf, L. V., Hu, D. H., Zhang, J. G., Graff, G. L., Liu, J., Pope, M. A., & Aksay, I. A. (2010). *ACS Nano*, 4, 1587.

[70] Guo, J. J., Li, Y., Zhu, S. M., Chen, Z. X., Liu, Q. L., Zhang, D., Moonc, W-J., & Song, D-M. (2012). *RSC Advances*, 2, 1356-1363.

[71] Hu, H., Wang, X., Liu, F., Wang, J., & Xu, C. (2011). *Synth. Met.*, 161, 404.

[72] Cao, A. N., Liu, Z., Chu, S. S., Wu, M. H., Ye, Z. M., Cai, Z. W., Chang, Y. L., Wang, S. F., Gong, Q. H., & Liu, Y. F. (2010). *Adv. Mater.*, 22, 103.

[73] Jia, L., Wang, D. H., Huang, Y. X., Xu, A. W., & Yu, H. Q. (2011). *J. Phys. Chem. C*, 115, 11466-11473.

[74] Li, Q., Guo, B., Yu, J., Ran, J., Zhang, B., Yan, H., & Gong, J. (2011). *J. Am. Chem. Soc.*, 133, 10878.

[75] Nethravathi, C., Nisha, T., Ravishankar, N., Shivakumara, C., & Rajamathi, M. (2009). *Carbon*, 47, 2054.

[76] Wu, J. L., Bai, S., Shen, X. P., & Jiang, L. (2010). *Appl. Surf. Sci.*, 257, 747.

[77] Ye, A. H., Fan, W. Q., Zhang, Q. H., Deng, W. P., & Wang, Y. (2012). *Catal. Sci. Technol.*, 2, 969-978.

[78] Li, Y. G., Wang, H. L., Xie, L. M., Liang, Y. Y., Hong, G. S., & Dai, H. J. (2011). *J. Am. Chem. Soc.*, 133, 7296-7299.

[79] Gao, E. P., Wang, W. Z., Shang, M., & Xu, J. H. (2011). *Phys. Chem. Chem. Phys.*, 13, 2887.

[80] Mukherji, A., Seger, B., Lu, G. Q., & Wang, L. Z. (2011). *ACS Nano*, 5, 3483.

[81] Ng, Y. H., Iwase, A., Kudo, A., & Amal, R. (2010). *J. Phys. Chem. Lett.*, 1, 2607.

[82] Zhang, X. F., Quan, X., Chen, S., & Yu, H. T. (2011). *Appl. Catal.*, B105, 237.

[83] Zhou, F., Shi, R., & Zhu, Y. F. (2011). *J. Mol. Catal. A: Chem.*, 340, 77.

[84] Geng, X. M., Niu, L., Xing, Z. Y., Song, R. S., Liu, G. T., Sun, M. T., Cheng, G. S., Zhong, H. J., Liu, Z. H., Zhang, Z. J., Sun, L. F., Xu, H. X., Lu, L., & Liu, L. W. (2010). *Adv. Mater.*, 22, 638.

[85] Zhang, H., Fan, X. F., Quan, X., Chen, S., & Yu, H. T. (2011). *Environ. Sci. Technol.*, 45, 5731.

[86] Zhu, M. S., Chen, P. L., & Liu, M. H. (2011). *ACS Nano*, 5, 4529.

[87] Xiang, Q. J., Yu, J. G., & Jaroniec, M. (2011). *J. Phys. Chem.*, C115, 7355-7363.

[88] Liao, G. Z., Chen, S., Quan, X., Yu, H. T., & Zhao, H. M. (2012). *J. Mater. Chem.*, 22, 2721.

[89] Wojtoniszak, M., Zielinska, B., Chen, X. C., Kalenczuk, R. J., & Borowiak-Palen, E. (2012). *J. Mater. Sci.*, 47(7), 3185-3190.

[90] Farhangi, N., Chowdhury, R. R., Medina-Gonzalez, Y., Ray, M. B., & Charpentier, P. A. (2011). *Appl. Catal. B: Environmental*, 110, 25-32.

[91] Zhang, Q., He, Y. Q., Chen, X. G., Hu, D. H., Li, L. J., Yin, T., & Ji, L. L. (2011). *Chin. Sci. Bull.*, 56, 331.

[92] Bell, N. J., Yun, H. N., Du, A. J., Coster, H., Smith, S. C., & Amal, R. (2011). *J. Phys. Chem.*, C115, 6004.

[93] Paek, S. M., Yoo, E., & Honma, I. (2009). *Nano Lett.*, 9, 72.

[94] Zhang, X. Y., Sun, Y. J., Li, H. P., Cui, X. L., & Jiang, Z. Y. (2012). *Inter. J. Hydrogen Energy*, 37, 811.

[95] Wang, P., Zhai, Y. M., Wang, D. J., & Dong, S. J. (2011). *Nanoscale*, 3, 1640.

[96] Shen, J. F., Yan, B., Shi, M., Ma, H. W., Li, N., & Ye, M. X. (2011). *J. Mater. Chem.*, 21, 3415.

[97] Shen, J. F., Shi, M., Yan, B., Ma, H. W., Li, N., & Ye, M. X. (2011). *Nano Res.*, 4(8), 795-806.

[98] Ding, S. J., Chen, J. S., Luan, D. Y., Boey, F. Y. C., Madhavi, S., & Lou, X. W. (2011). *Chem. Commun.*, 47, 5780.

[99] Li, N., Liu, G., Zhen, C., Li, F., Zhang, L. L., & Cheng, H. M. (2011). *Adv. Funct. Mater.*, 21, 1717.

[100] Zhu, C. Z., Guo, S. J., Wang, P., Xing, L., Fang, Y. X., Zhai, Y. M., & Dong, S. J. (2010). *Chem. Commun.*, 46, 7148.

[101] Lambert, T. N., Chavez, C. A., Hernandez-Sanchez, B., Lu, P., Bell, N. S., Ambrosini, A., Friedman, T., Boyle, T. J., Wheeler, D. R., & Huber, D. L. (2009). *J. Phys. Chem.*, C113, 19812.

[102] Guo, J., Zhu, S., Chen, Z., Li, Y., Yu, Z., Liu, Q., Li, J., Feng, C., & Zhang, D. (2011). *Ultrason. Sonochem.*, 18, 1082.

[103] Yu, J. G., Zhang, J., & Jaroniec, M. (2010). *Green Chem.*, 12, 1611.

[104] Yu, J. G., & Ran, J. R. (2011). *Energy Environ. Sci.*, 4, 1364.

[105] Qi, L. F., Yu, J. G., & Jaroniec, M. (2011). *Phys. Chem. Chem. Phys.*, 13, 8915.

[106] Li, Q. Y., & Lu, G. X. (2007). *J. Mol. Catal.*, (China), 21, 590-598.

[107] Yu, C. L., & Yu, J. C. (2009). *Catal. Lett.*, 129, 462-470.

[108] Bell, N. J., Ng, Y. H., Du, A., Coster, H., Smith, S. C., & Amal, R. (2011). *J. Phys. Chem.*, C115, 6004-6009.

[109] Lv, X. J., Fu, W. F., Chang, H. X., Zhang, H., Cheng, J. S., Zhang, G. J., Song, Y., Hub, C. Y., & Li, J. H. (2012). *J. Mater. Chem.*, 22, 1539-1546.

[110] Yu, J. C., Yu, J. G., Ho, W. K., Jiang, Z. T., & Zhang, L. Z. (2002). *Chem. Mater.*, 14, 3808.

[111] Yu, J. G., Wang, W. G., Cheng, B., & Su, B. L. (2009). *J. Phys. Chem. C*, 113, 6743.

[112] Zhang, H., Lv, X., Li, Y., Wang, Y., & Li, J. (2010). *ACS Nano*, 4, 380-386.

IntechOpen